EPiC Series in Computing

Volume 104, 2024, Pages 109–125

Proceedings of 3rd International Workshop on
Mathematical Modeling and Scientific Computing

Non-integer Approach to Modelling Compartments of Cardiovascular Circulatory System

Iva Janković[1] and Mirna Kapetina Radović[1]

University of Novi Sad, Faculty of Technical Sciences, Novi Sad, Serbia
iva.jankovic@uns.ac.rs,mirna.kapetina@uns.ac.rs

Abstract

For predicting cardiovascular diseases, mathematical modelling of the cardiovascular system has been proven to be a powerful asset. The governing idea is to analyse it through compartments as multiple connected subsystems with inputs and outputs. In this paper, models were identified for four subsystems of input-output sequence (left ventricle - left atrium - ascending aorta - descending aorta - left common carotid artery) by modelling frequency response. The data set used for model identification consisted of blood pressure during four consecutive heart contractions of four circulatory segments from clinical trials performed on a pig. The goal is to discover a linear model with a non-integer order that succinctly represents the process, outperforming high-order autoregressive exogenous input (ARX) integer models. This model identification occurs non-parametrically, aiming to achieve the best smooth fit in the frequency domain by minimizing the difference between real measurements and model predictions using the particle swarm optimization (PSO) algorithm.

1 Introduction

Since being introduced as a tool for modeling tissue viscoelasticity [2], fractional calculus (FC) has been recognised as a powerful apparatus in modelling and control of numerous engineering systems. Given that living organisms are among the most complex systems known, FC found its use in medicine and biology.

Fractional modelling in medical research. Due to its non-local properties and necessity of a know-how approach in medical research, FC has been greatly utilised for biomedical phenomena. For example, the branch of fractional mathematical oncology offers various options for modelling response to treatment, potential tumour growth, metastasis etc. as shown in [18].

The importance of tumor mathematical models is reflected in the need for a better understanding of cancer proliferation and, consequently, more personalized and efficient treatment. When it comes to tumour growth modelling, superiority of fractional order models over integer order equivalents has been shown on multiple commonly used models. Namely, in one study [1], mean squared error of fractional order models was reduced by at least half when compared to integer equivalents.

V.L. Turova, A.E. Kovtanyuk and J. Zimmer (eds.), MMSC 2024 (EPiC Series in Computing, vol. 104), pp. 109–125

Overall, fractional order generalisation of classical mathematical models is demonstrating huge potential. In addition, to accentuate specific features of cancer dynamics, integration of control theory and mixing stochastic and fractional calculus are proposed and therefore represent a new direction towards finding a suitable model to describe various cancer.

Although fractional mathematical oncology does represent a booming area of FC application, modelling healthy tissues and organ systems as basis for understanding pathologies is also a significant part of research on non-integer mathematical modelling.

For example, two main characteristics that make the respiratory system suitable for FC are geometric structure from which an electrical analogue can be derived, and tissue structure (the viscoelasticity of lung parenchyma), from which an mechanical analogue can be derived.

In this case, classical integer-order modelling resulted in a very high-order impedance model, while low-order fractional order model performed accurately over the range of frequencies significant for the respiratory system. That model can be used for understanding the pathophysiological mechanism of pulmonary diseases and their diagnosis more easily [6]. In addition, the fractal nature of certain structures and organ structure-function relation is better understood due to their connection to FC. In the respiratory system, structure of pulmonary tree is linked with lung tissue mechanics in way easily describable with FC as shown in [5].

Modelling of cardiovascular system. In modeling macrocirculation, lumped parameter models are often preferred over distributed models because they showcase the complexity of the cardiovascular system (CVS) while relying on a minimal set of parameters. However, it is important to note that these models do not account for the anatomical layout of the vessels and, therefore, cannot represent certain characteristics.

One of the most popular models is two-element WindKessel (WK) model and its modifications. It depicts systemic vascular circuit in which capacity describes the intake of blood volume into the arterial system as a response to the increase of pressure, and resistance represents relation between reduction in average pressure from the arterial side to the venous side and cardiac output [4]. The importance of these models is reflected in their wide usage in predicting cardiovascular pathologies. Studies have shown the reliability of WK models for estimating blood pressure by predicting arterial blood pressure waveform [15, 20].

In addition, it is common to use multi-compartment lumped models for modelling the cardiovascular network because of its computational efficiency which creates space for potential patient-specific modelling. There is a variety of information that can be gained by adding elements that represent compartments where pathologies can be detected. For example, authors in [17] opted for extension of classical WK model when modelling atherosclerosis as one of the main risk factors for cardiovascular diseases.

The aim of the paper is to question whether the fractional or integer model is more suitable for representing the dynamics between compartments of the cardiovascular circulatory system. By obtaining frequency-domain characteristics of the discrete-time model of sufficiently high order, the structure of the fractional-order model can be identified. This suggests that the appropriate model structure is not known in advance. Unknown model parameters are obtained through non-parametric frequency-domain identification by minimizing the difference between actual measurements and predictions using the particle swarm optimization (PSO) algorithm.

The paper is organized as follows. Section 2 gives an overview of cardiovascular circulatory system and its compartments. Within Section 3 the identification and modeling approaches carried out for both integer and fractional models are explained. By comparing simulation results and experimental data, model's capabilities are examined as explained in Section 4. Finally, in Section 5, conclusions are drawn.

2 Compartments of cardiovascular circulatory system

The main function of the cardiovascular circulatory system is to provide blood supply to all the parts of a body. In the blood, oxygen and nutrients among other substances are distributed and,therefore, the cardiovascular system represents vital system of organs. Besides blood, the CVS consists out of heart and blood vessels. Within the system, two types of circulation i.e. loops are present. Systemic circulation transports oxygenated blood from the heart to the rest of the body and returns deoxygenated one back to the heart. In addition to systemic circulation, pulmonary circulation exists to oxygenate blood by transporting it through the lungs.

2.1 Blood flow in CVS

The heart directs blood flow through the aorta for systemic circulation or through the pulmonary artery for pulmonary circulation, thereby connecting the two circulations. Through the pulmonary veins, oxygenated blood enters the heart. When it contracts, blood is squeezed from the left atrium to the left ventricle throughout the mitral valve. The thickest chamber in heart, the left ventricle, generates force to push the blood into the biggest artery in human body, the aorta.

The part of aorta directly connected i.e. the upward portion of aortic arch is the ascending aorta. Afterwards, one portion of the blood is directed towards neck and head via left common carotid artery and two other arteries and rest of it continues to flow into the descending aorta. It supplies blood to major abdominal organs (via the abdominal aorta) and some organs within the thorax (via the thoracic aorta) [3].

In Figure 1 blood flow between the compartments of interest in this paper is shown. In addition, numeration of the subsystems that will be described in Section 2.2 is marked. It is important to note that types of vessels used in this paper, arteries, receive the highest blood flow pressure and have high pressure values.

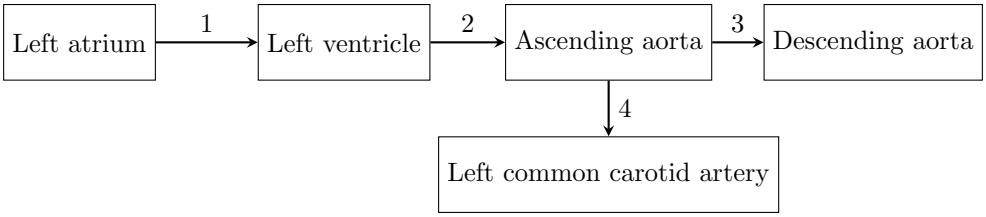

Figure 1: Blood flow throughout the observed compartments with marked subsystems.

2.2 Blood pressure in CVS

Blood pressure (BP) represents force per unit area that blood exerts on the walls of blood vessels, and its value is determined by relative distance from the aortic arch and time [13]. Unlike blood flow, BP can be used directly for detecting a number of medical conditions such as arrhythmia, hypovolemia etc.

The connection between two quantities is the stretch of the walls of the arteries by the volume they contain. The slope of the pressure–flow line and its relevance has been thoroughly explained in [12]. In this paper, the authors have chosen blood pressure as a quantity representing the input and the output of the compartment modeled due to its diagnostic value and simplicity.

Variations in systolic pressure among different cardiovascular compartments occur because of the compliance of the large arteries. The BP value also depends on the stage of the cardiac cycle observed. For example, ventricles and atriums experience greater change in volume during systole and diastole and therefore have bigger variation of BP throughout cardiac cycle [19].

3 Mathematical modelling

As previously mentioned, the aim is to determine the superiority of fractional order models over traditional integer-order models in representing the dynamics of the cardiovascular system. Fractional models, which allow for non-integer differentiation, are particularly appealing due to their ability to model systems with memory and hereditary properties of physiological systems that are often missed by integer-order models. They enable modeling of systems with non-local memory effects and a more flexible response to inputs.

One of the key advantages of fractional-order models is their capacity to represent frequency responses that are not restricted to integer multiples of the standard 20 dB/decade slope seen in integer-order systems [14]. In traditional integer-order systems, the Bode plot slopes are integer multiples of 20 dB/decade for each pole or zero. However, fractional-order systems exhibit slopes that can vary continuously, reflecting more complex dynamics and allowing for a finer-grained analysis of system behavior [16]. To validate the effectiveness of fractional models, an integer-order model is first identified and used as a baseline for comparison.

In this case, an integer-order discrete-time ARX model is used due to its ability to provide a non-parametric identification of the system without imposing a predefined model structure [11]. The non-parametric identification performed with the ARX model is advantageous because it eliminates the need to impose constraints based on prior assumptions about model structure.

Once the ARX model is identified, its frequency characteristics are analyzed, which helps derive the structure of the fractional-order model. Fractional models, characterized by non-integer derivatives, often provide a more nuanced representation of real-world systems that exhibit memory and hereditary properties.The approach to mathematical modelling taken in the paper has been thoroughly explained in [8, 9], but essential steps are:

1. **Identifying discrete-time high-order ARX model.** A high-order ARX model is developed to fit time-domain data accurately while minimizing sensitivity to disturbances.

2. **Determining the structure of fractional model by analysing frequency characteristic of previously obtained ARX model.** The frequency characteristics of the ARX model are analyzed to derive a fractional model structure that better captures the system's dynamics.

3. **Parameter identification using global optimization technique such as PSO algorithm.** The fractional model's parameters are estimated by fitting both the magnitude and phase characteristics of the system, utilizing the PSO algorithm.

In the following subsections, steps towards obtaining the fractional model have been described in more detail.

3.1 Integer order model identification

The first step involves identifying a discrete-time high-order optimal ARX model, which serves as an integer-order representation of the cardiovascular system. The general form of the ARX model is

$$A(q)y(k) = B(q)u(k-d) + e(k), \tag{1}$$

where $y(k)$ is the output at time k, $u(k-d)$ is the input signal delayed by d time steps. $e(k)$ is the error or disturbance term, $A(q)$ and $B(q)$ are polynomials in the forward shift operator q of orders n and $n-1$ where n is empirically chosen to be sufficiently large. The parameters of the ARX model structure are estimated using the least squares method.

By using high-order ARX models, fitting time-domain data is performed while preventing issues related to sensitivity to noise and disturbances. In particular, high-order models are well-suited for over-parameterized situations, where the goal is to fit time-domain data with high accuracy. However, this model is an intermediate step toward obtaining the fractional model. Therefore, the ARX structure is deliberately over-parameterized to ensure sufficient flexibility.

3.2 Non-integer identification, frequency analysis and optimization

The process of non-integer (fractional) modeling begins by analyzing the frequency characteristics of the previously obtained high-order integer ARX model, $G_{ARX}(j\omega)$. This analysis is crucial for understanding the system's dynamics in the frequency domain. ARX models offer a regularized representation of the system's frequency response, providing a structured and stable framework for analysis.

While theoretically possible, determining frequency characteristics by computing the ratios of Fourier transforms of the output and input is often numerically unstable and impractical. The ARX model helps avoid these issues by offering a reliable estimate of the system's frequency response. Based on the frequency characteristics derived from the ARX model, we hypothesize a fractional-order model designed to match the same frequency response. This model leverages insights from the ARX analysis to accurately capture the system's dynamics with fractional-order flexibility, offering a more precise and interpretable representation compared to direct Fourier transform-based approaches.

By examining the Bode diagrams of $G_{ARX}(j\omega)$, we can postulate the structure of the fractional model. Typically, the Bode plots reveal critical frequencies with slopes that deviate from integer multiples of the standard 20 dB/decade. We discard non-physiological values to focus on the relevant characteristics for the cardiovascular system. The Bode diagrams also allow us to approximate the number of slope changes, which indicates the potential number of poles and zeros in the system needed to fit the observed frequency response.

In fractional-order models, the effects of poles and zeros on the slope differ from that in integer-order models. Each pole typically causes a decrease in slope by α $\times$20 dB/decade, where α is the fractional order of the pole. Conversely, each zero causes an increase in slope by α $\times$20 dB/decade. This continuous variation in slopes, rather than discrete changes, reflects the more nuanced dynamics captured by fractional-order models.

After assuming the structure of the fractional model $G_{FO}(j\omega)$, the next step is to estimate its parameters. The goal is to ensure that the frequency response of the fractional-order model aligns closely with that of the ARX model in the frequency region of interest. This alignment ensures that the fractional model accurately represents the system's dynamics in the ARX model.

To achieve this, we employ optimization techniques to fit the fractional model's parameters such that the magnitude and phase characteristics of $G_{FO}(j\omega)$ closely match those of $G_{ARX}(j\omega)$ in the frequency region of interest. This process involves minimizing a cost function that quantifies the discrepancy between the fractional and ARX model responses:

$$\begin{aligned} J = &\sum_{\omega=\omega_{min}}^{\omega_{max}} |20_{10}\log\left(|G_{FO}(j\omega,p)|\right) - 20\log\left(|G_{ARX}(j\omega,p)|\right)| \\ &+ \sum_{\omega=\omega_{min}}^{\omega_{max}} |\angle G_{FO}(j\omega,p) - \angle G_{ARX}(j\omega,p)| + 1000\sum_{i=1}^{n}(p<0). \end{aligned} \tag{2}$$

The cost function consists of three components: first, the magnitude discrepancy, which is the sum of the absolute differences in the magnitude (in dB) between the two models over the frequency range from $\omega_{\min} = 0.1\,\text{rad/s}$ to $\omega_{\max} = 100\,\text{rad/s}$; second, the phase discrepancy, which measures the absolute difference between the phase of the two models over the same frequency range; and third, a penalty term that applies a large penalty (1000) when any of the parameters p of the fractional model $G_{FO}(j\omega,p)$ is negative, ensuring physically meaningful solutions. The angular frequencies ω are distributed uniformly on a logarithmic scale in the range from $\omega_{\min} = 0.1\,\text{rad/s}$ to $\omega_{\max} = 100\,\text{rad/s}$, with $N = 100$ points. The parameter n represents the number of parameters of the fractional model. Given the complex and non-convex nature of the problem, a global optimization algorithm is employed. Specifically, a variant of the Particle Swarm Optimization (PSO) algorithm, known as Generalized PSO (GPSO), is used as described in [7].

3.2.1 Generalized particle swarm optimization

The main objective of PSO is to explore the search space using a swarm of particles, each representing a potential solution, [10]. Each particle is characterized by its current position $x[k]$ and velocity $v[k]$, the latter being the difference between the current and previous positions. Initially, positions and velocities are randomly assigned.

At each iteration, particles update their positions based on two key values: the particle's personal best (pbest) $p[k]$ and the swarm's global best (gbest) $g[k]$. The new velocity for each particle is calculated as:

$$v[k+1] = w\cdot v[k] + cp\cdot rp[k](p[k]-x[k]) + cg\cdot rg[k](g[k]-x[k]), \tag{3}$$

where w, cp, and cg represent the inertial, cognitive, and social components, and rp and rg are random numbers in the range $[0,1]$. The particle's position is updated by: $x[k+1] = x[k] + v[k+1]$.

Here, the Generalized PSO (GPSO) algorithm is used. GPSO is inspired by linear control theory, and the swarm is treated as a second-order dynamical system. The position update is:

$$x[k+1] = 2\zeta\rho x[k] - \rho^2 x[k-1] + \left(1-2\zeta\rho+\rho^2\right)(cp[k] + (1-c)g[k]), \tag{4}$$

where ρ is the damping factor (decreasing from 0.95 to 0.6, as noted in [7]), and ζ is an oscillation factor, randomly selected from $[-0.9, 0.6]$. In this study, the GPSO proposed in [7] is used to obtain optimal parameters for a fractional-order model that accurately fits the frequency characteristics of the cardiovascular system. The algorithm explores the parameter space, adjusting the fractional-order model's parameters to minimize the error between the model's frequency response and the target frequency characteristics. GPSO operates in an n-dimensional space, providing flexibility and control through its damping factor ρ and oscillation factor ζ, ensuring model achieves the desired fit.

4 Results

4.1 Database description

Since pigs and humans have similar cardiovascular anatomy, experimental data from a clinical trial on a pig, as described in [17], was used for the system's input and output signals. In this trial, pressure values were measured for left ventricular pressure $LVP(t)$ (mmHg), left atrial pressure $LAP(t)$ (mmHg), descending aorta pressure $AP(t)$(mmHg), ascending aorta pressure $AoP(t)$ (mmHg), and left common carotid artery pressure $LCP(t)$ (mmHg).

All signals were recorded with a sample time of 4 ms, and each time series covers 4.5 seconds. Due to the relatively short duration of the data for robust system identification, all signals were duplicated to extend their length, enabling better observation of the system's behavior. The data represent the normal steady-state behavior of the pig's cardiovascular system.

Since the focus of the linear model is on signal variations rather than the specific working point, the offset was removed, as the working point itself was not crucial for this stage of the analysis. In Figure 2, the experimental data is shown as input (blue line) and output (orange line) signals of four subsystems in the time domain.

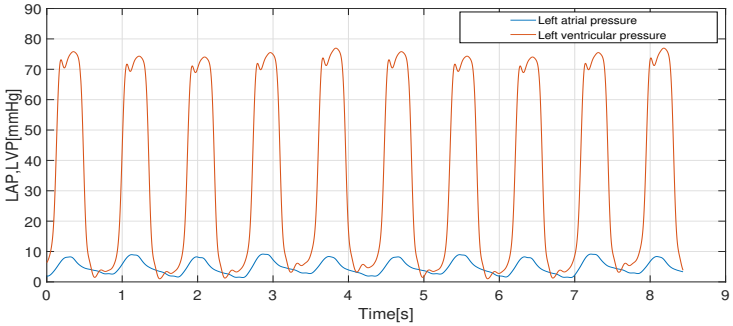

(a) Left atrium - left ventricle subsystem.

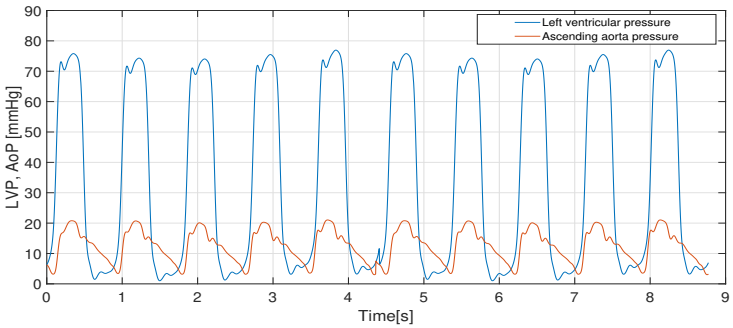

(b) Left ventricle - ascending aorta subsystem.

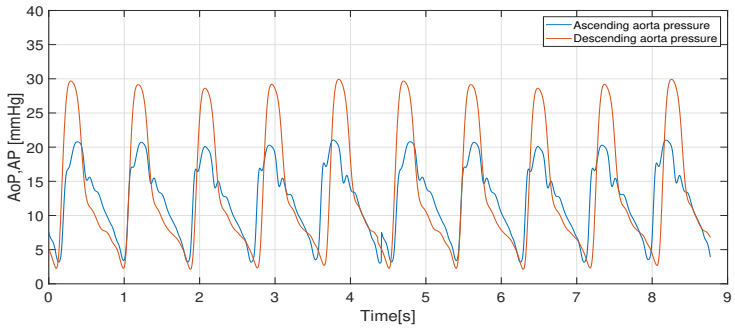

(c) Ascending aorta-descending aorta subsystem.

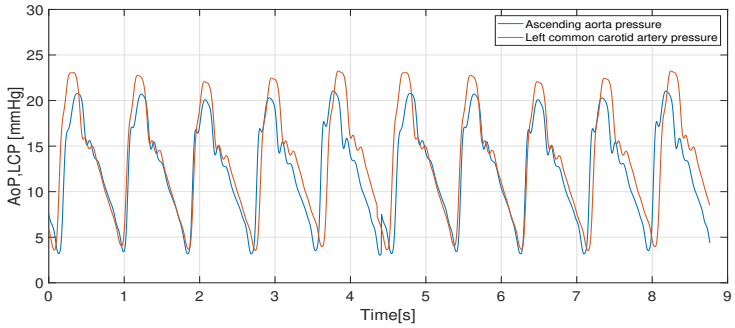

(d) Ascending aorta-left common carotid artery subsystem.

Figure 2: Experimental data as input and output signals of subsystem.

4.2 Model identification overview

As previously described, the ARX identification algorithm is applied to pairs of input and output signals from the dataset that represent different subsystems of the cardiovascular system. In the data preprocessing stage, the output signal was manually shifted and aligned with the input signal, thereby setting the delay parameter d explicitly. This adjustment allowed us to simplify the identification process by removing the need to estimate an additional delay during the ARX model fitting. Consequently, during the ARX identification procedure outlined in Subsection 3.1 and implemented in the MATLAB software package, the lag parameter d was fixed at zero, enabling a focus solely on optimizing the parameters na and nb for model accuracy. The results for ARX models across four subsystems are summarized in Table 1, where the model fit to the estimation data, the final prediction error (FPE), and the mean squared error (MSE) are reported as indicators of the model's performance.

In the subsequent analysis, we present the results for each subsystem, beginning with the parameters of the identified high-order ARX models. The frequency response of these ARX models is analyzed to inform the formulation of fractional-order model structures. Based on the observed slopes and behavior, the fractional-order models are derived. Parameter identification for the fractional models is conducted using a PSO algorithm with a particle swarm size of 200 and a maximum of 1000 iterations. These steps, implemented in MATLAB, produce the final results for each subsystem.

Subsystem	n	Delay in samples (approximate seconds)	Fit to estimation data	FPE	MSE
(1) Left atrium - left ventricle	8	64 ($\approx$ 0.256 sec)	72.43%	0.0179	72.7
(2) Left ventricle - ascending aorta	9	13 ($\approx$ 0.052 sec)	53.11%	0.0665	6.3
(3) Ascending aorta - descending aorta	15	13 ($\approx$ 0.052 sec)	56.68%	0.0167	14.7
(4) Ascending aorta - left carotid artery	8	15 ($\approx$ 0.06 sec)	54.64%	0.0365	7.1

Table 1: ARX models parameters. Note: The column with delay is calculated during the data preparation process.

Note: The ARX model's linear nature does not fully account for nonlinear dynamics, which introduces some error, especially around signal peaks. This trade-off results in a mean squared error (MSE) that, although relatively high, is reasonable given the context. The model still satisfactorily captures the essential shape and trend of the data, offering a balance between simplicity and practical interpretability.

4.2.1 Subsystem 1: left atrium - left ventricle

Considering the discrete-time representation (1) of ARX model given in previous section, the polynomials A and B for subsystem 1 are:

$$A(z) = 1 - 4.687z^{-1} + 7.76z^{-2} - 4.439z^{-3} - 1.52z^{-4} + 1.333z^{-5} + 1.987z^{-6} - 1.961z^{-7},$$
$$B(z) = 3.31 - 15.43z^{-1} + 25.65z^{-2} - 14.24z^{-3} - 5.092z^{-4} + 4.342z^{-5} + 6.3z^{-6} - 6.404z^{-7}.$$

The optimal ARX model is obtained with 20 parameters in total. In Figure 3a comparison between the time-domain responses provided by the ARX model and experimental data is given. By observing relevant part of frequency characteristic of the ARX model as seen in Fig. 3b the following model structure is obtained:

$$G(s) = k\frac{\left(\frac{s}{\omega_1}+1\right)^{\alpha_1}}{\left(\frac{s}{\omega_2}+1\right)^{\alpha_2}}, \tag{5}$$

in which model parameters ω_1, ω_2 are critical frequencies and corresponding orders α_1, α_2 with their values given in Table 2 and frequency characteristic of both models in Fig. 4.

k	α_1	ω_1	α_2	ω_2
19.269064	1.172491	15.153801	1.687439	41.783736

Table 2: Optimal parameters of the fractional-order model (fitness function from eq. (2), $J = 16.1859$).

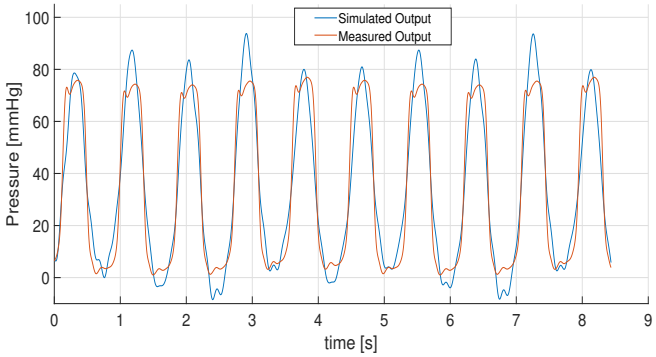

(a) Time-domain response comparison between ARX model and experimental data.

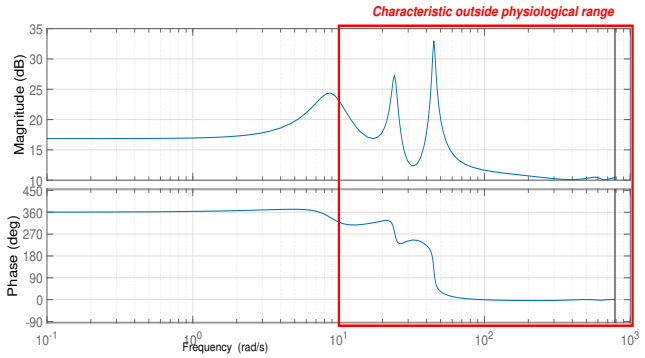

(b) Frequency characteristic of the ARX model.

Figure 3: ARX model results for subsystem 1.

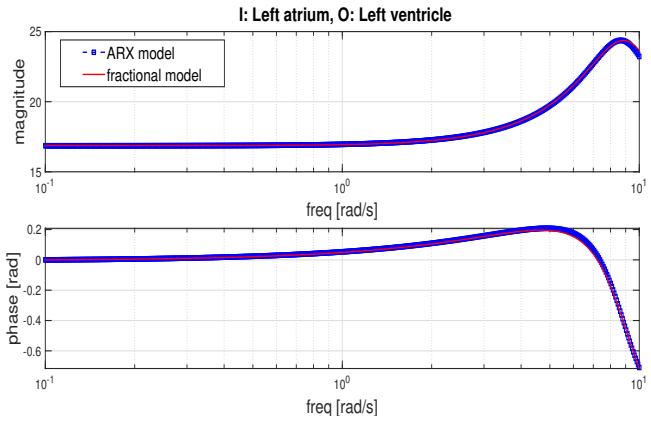

Figure 4: Frequency-domain comparison between ARX and fractional-order model.

4.2.2 Subsystem 2: left ventricle - ascending aorta

Considering the discrete-time representation (1) of ARX model given in previous section, the polynomials A and B for subsystem 2 are:

$$A(z) = 1 - 2.932z^{-1} + 2.484z^{-2} - 0.1646z^{-3} - 0.186z^{-4} - 0.2255z^{-5} - 0.158z^{-6} + 0.1517z^{-7} + 0.05983z^{-8} - 0.02952z^{-9},$$

$$B(z) = 0.436 - 1.4z^{-1} + 1.344z^{-2} - 0.1411z^{-3} - 0.1494z^{-4} - 0.1719z^{-5} - 0.1217z^{-6} + 0.3143z^{-7} - 0.1096z^{-8}.$$

The optimal ARX model is obtained with 18 parameters in total. In Figure 5a comparison between the time-domain responses provided by the ARX model and experimental data is given. By observing relevant part of frequency characteristic of the ARX model as seen in Fig. 5b the following model structure is obtained:

$$G(s) = k\frac{\left(\frac{s}{\omega_1}+1\right)^{\alpha_1}}{\left(\frac{s}{\omega_2}+1\right)^{\alpha_2}\left(\frac{s}{\omega_3}+1\right)^{\alpha_3}},$$

in which unknown model parameters ω_1, ω_2 are critical frequencies and corresponding orders α_1, α_2 with their values given in Table 3 and relevant frequency characteristic of both models in Fig. 6.

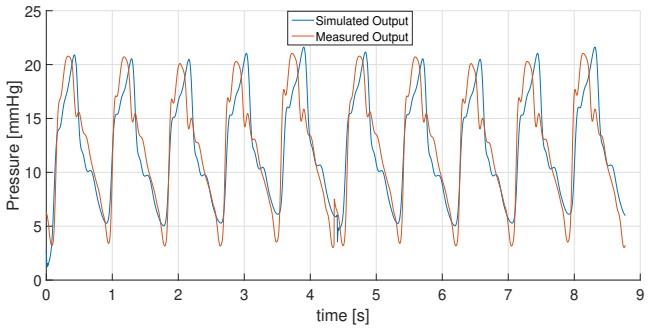

(a) Time-domain response comparison between ARX model and experimental data.

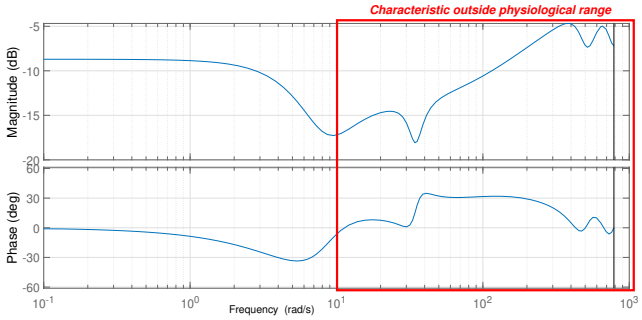

(b) Frequency characteristic of the ARX model.

Figure 5: ARX model results for subsystem 2.

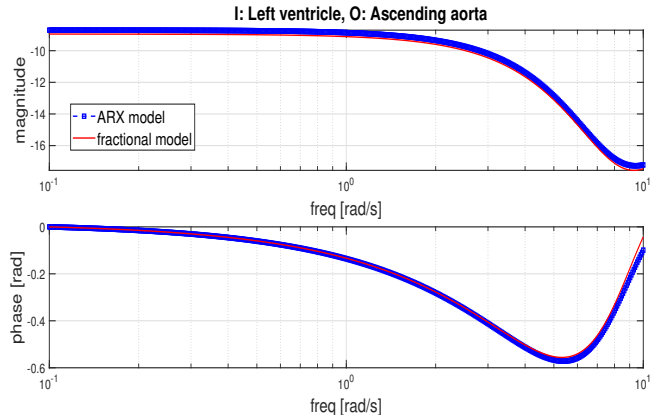

Figure 6: Frequency-domain comparison between ARX and fractional-order model.

k	α_1	ω_1	α_2	ω_2	α_3	ω_3
1.822428	1.566772	30.633108	0.820903	17.787691	1.160627	8.535039

Table 3: Optimal parameters of the fractional-order model (fitness function from eq. (2), $J = 7.831$).

4.2.3 Subsystem 3: ascending aorta - descending aorta

Considering the discrete-time representation (1) of ARX model given in previous section, the polynomials A and B for subsystem 3 are:

$$\begin{aligned} A(z) = 1 &- 3.251z^{-1} + 3.078z^{-2} - 0.2822z^{-3} - 0.3753z^{-4} - 0.07941z^{-5} - 0.2257z^{-6} \\ &- 0.08923z^{-7} + 0.08502z^{-8} + 0.09687z^{-9} + 0.01037z^{-10} + 0.2238z^{-11} \\ &- 0.1979z^{-12} + 0.1562z^{-13} - 0.285z^{-14} + 0.1357z^{-15}, \end{aligned}$$

$$\begin{aligned} B(z) = 0.4888 &- 1.6z^{-1} + 1.542z^{-2} - 0.1624z^{-3} - 0.195z^{-4} - 0.04065z^{-5} - 0.1073z^{-6} \\ &- 0.04306z^{-7} + 0.04778z^{-8} + 0.06468z^{-9} + 0.003471z^{-10} + 0.1286z^{-11} \\ &- 0.1059z^{-12} - 0.07725z^{-13} + 0.05664z^{-14}. \end{aligned}$$

The optimal ARX model is obtained with 30 parameters in total. In Figure 7a comparison between the time-domain responses provided by the ARX model and experimental data is given. By observing relevant part of frequency characteristic of the ARX model as seen in Fig. 7b following model structure 5 is obtained. Parameter values are given in Table 4 and relevant frequency characteristic of both models in Fig. 8.

k	α_1	ω_1	α_2	ω_2
2.913022	1.120432	27.740819	1.671349	75.516957

Table 4: Optimal parameters of the fractional-order model (fitness function from eq. (2), $J = 20.0913$).

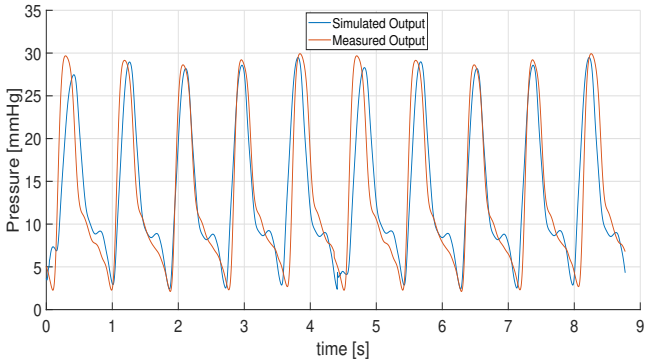

(a) Time-domain response comparison between ARX model and experimental data.

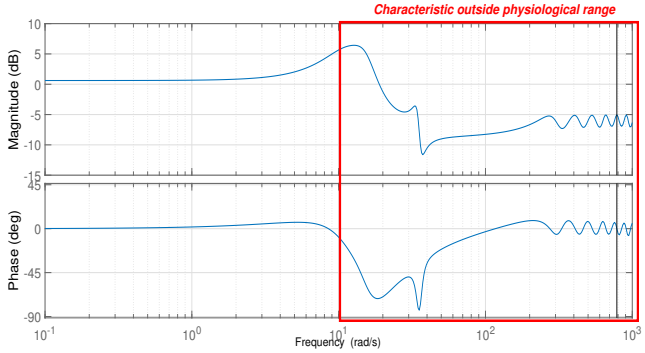

(b) Frequency characteristic of the ARX model.

Figure 7: ARX model results for subsystem 3.

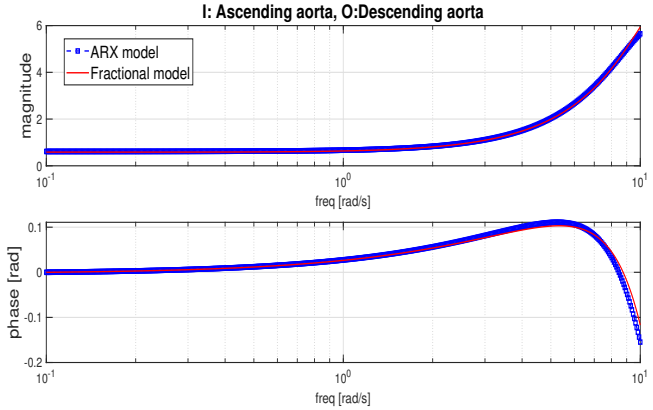

Figure 8: Frequency-domain comparison between ARX and fractional-order model.

4.2.4 Subsystem 4: ascending aorta - left common carotid artery

Considering the discrete-time representation (1) of ARX model given in previous section, the polynomials A and B for subsystem 4 are:

$$\begin{aligned} A(z) &= 1 - 3.513z^{-1} + 3.795z^{-2} - 0.7534z^{-3} - 0.6673z^{-4} - 0.5986z^{-5} + 0.6984z^{-6} \\ &\quad + 0.05848z^{-7} - 0.1193z^{-8}, \\ B(z) &= 0.556 - 1.985z^{-1} + 2.267z^{-2} - 0.4822z^{-3} - 0.4268z^{-4} - 0.3845z^{-5} \\ &\quad + 0.6625z^{-6} - 0.2069z^{-7}. \end{aligned}$$

The optimal ARX model is obtained with 16 parameters in total. In Figure 9a comparison between the time-domain responses provided by the ARX model and experimental data is given. By observing relevant part of frequency characteristic of the ARX model as seen in Fig. 9b the following model structure is obtained:

$$G(s) = k \frac{\left(\frac{s}{\omega_1} + 1\right)^{\alpha_1} \left(\frac{s}{\omega_2} + 1\right)^{\alpha_2}}{\left(\frac{s}{\omega_3} + 1\right)^{\alpha_3} \left(\frac{s}{\omega_4} + 1\right)^{\alpha_4}}, \tag{6}$$

in which unknown model parameters $\omega_1, \omega_2, \omega_3, \omega_4$ are critical frequencies and corresponding orders $\alpha_1, \alpha_2, \alpha_3, \alpha_4$ with their values given in Table 5 and relevant frequency characteristic of both models in Fig. 10.

k	α_1	ω_1	α_2	ω_2	α_3	ω_3	α_4	ω_4
1.252332	1.015567	22.017415	0.989481	7.277634	1.323887	33.682557	0.966054	5.537856

Table 5: Optimal parameters of the fractional-order model (fitness function from eq. (2), $J = 2.983$).

5 Conclusion

The complexity of the cardiovascular system necessitates the development of sophisticated models for simulating cardiovascular diseases. Our research introduces a simplified fractional-order model that builds upon traditional models, enhancing cardiovascular simulations and offering valuable insights into conditions such as atherosclerosis, hypertension, heart failure, and arterial stiffness.

The strength of this fractional-order model lies in its simplicity and interpretability, making it more practical for real-time monitoring and clinical applications compared to more complex models. This model serves as a foundational tool for understanding cardiovascular dynamics and supports further research and development. Its effectiveness in simulating pathological conditions such as arrhythmias and the impact of various therapeutic interventions highlights its versatility and adaptability, establishing it as a significant asset for both research and clinical practice.

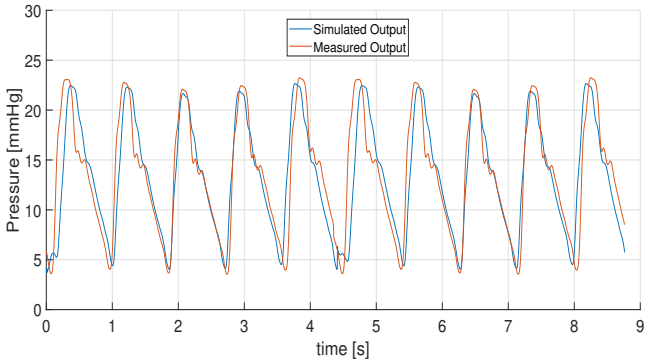

(a) Time-domain response comparison between ARX model and experimental data.

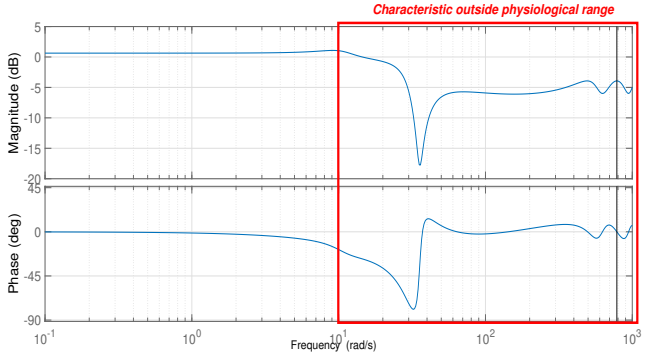

(b) Frequency characteristic of the ARX model.

Figure 9: ARX model results for subsystem 4.

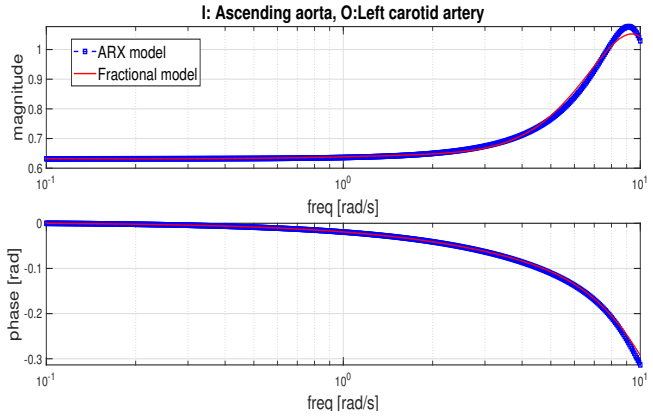

Figure 10: Frequency-domain comparison between ARX and fractional-order models.

6 Acknowledgments

This research has been supported by the project Chemobrain: Imaging biomarkers of neuronal injury and brain plasticity—ChemoBRAIN, No 7750129, Science Fund of the Republic of Serbia. and M.K.R has been supported by the Ministry of Science, Technological Development and Innovation (Contract No. 451-03-5/2024-03/200156) and the Faculty of Technical Sciences, University of Novi Sad (Project No. 01-3394/1).

References

[1] T. Alinei-Poiana, E. Dulf, and L. Kovacs. Fractional calculus in mathematical oncology. *Scientific Reports*, 13(1):10083, 2023.

[2] R. Bagley and P. Torvik. Fractional calculus - a different approach to the analysis of viscoelastically damped structures. *AIAA Journal*, 21(5):741–748, 1983.

[3] R. Chaudhry, J. H. Miao, and A. Rehman. Physiology, cardiovascular. In *StatPearls [https://www.ncbi.nlm.nih.gov/books/NBK493197/]*. StatPearls Publishing, 2022.

[4] T. C. Gasser. *Vascular Biomechanics*. Springer, 2021.

[5] C. Ionescu, A. Lopes, D. Copot, J. T. Machado, and J. H. Bates. The role of fractional calculus in modeling biological phenomena: A review. *Communications in Nonlinear Science and Numerical Simulation*, 51:141–159, 2017.

[6] C.M. Ionescu. *Fractional order models of the human respiratory system*. PhD thesis, Ghent University, 2009.

[7] Ž. Kanović, M. R. Rapaić, and Z. D. Jeličić. Generalized particle swarm optimization algorithm-theoretical and empirical analysis with application in fault detection. *Applied Mathematics and Computation*, 217(24):10175–10186, 2011.

[8] M. Kapetina. *Adaptivna estimacija parametara sistema opisanih iracionalnim funkcijama prenosa*. PhD thesis, University of Novi Sad, Faculty of Technical Sciences, Novi Sad, Serbia, 2017.

[9] M. Kapetina, P. Lino, G. Maione, and M. Rapaić. Estimation of non-integer order models to represent the pressure dynamics in common-rail natural gas engines. *IFAC-PapersOnLine*, 50(1):14551–14556, 2017.

[10] J. Kennedy and R. Eberhart. Particle swarm optimization. In *Proceedings of ICNN'95 - International Conference on Neural Networks*, volume 4, pages 1942–1948. IEEE, 1995.

[11] L. Ljung. *System Identification: Theory for the User*. Prentice Hall information and system sciences series. Prentice Hall PTR, 1999.

[12] S. Magder. The meaning of blood pressure. *Critical Care*, 22(1):257, 2018.

[13] T.G. Myers, V. Ribas Ripoll, A. Sáez de Tejada Cuenca, S. L. Mitchell, and M. J. McGuinness. Modelling the cardiovascular system for assessing the blood pressure curve. *Mathematics-in-industry case studies*, 8:1–16, 2017.

[14] K. Ogata. *Modern Control Engineering*. Instrumentation and controls series. Prentice Hall, 2010.

[15] M. Paisal, A. Sufyan, I. Taib, T. Arifin, N. Darlis, et al. An analysis of blood pressure waveform using windkessel model for normotensive and hypertensive conditions in carotid artery. *Journal of Advanced Research in Fluid Mechanics and Thermal Sciences*, 57(1):69–85, 2019.

[16] I. Podlubny. *Fractional Differential Equations: An Introduction to Fractional Derivatives, Fractional Differential Equations, to Methods of Their Solution and Some of Their Applications*. Elsevier, 1998.

[17] J. E. Traver, C. Nuevo-Gallardo, I. Tejado, J. Fernández-Portales, J. F. Ortega-Morán, J. B. Pagador, and B. M. Vinagre. Cardiovascular circulatory system and left carotid model: A fractional approach to disease modeling. *Fractal and Fractional*, 6(2):64, 2022.

[18] L.C. Vieira, R. S. Costa, and D. Valério. An overview of mathematical modelling in cancer research: Fractional calculus as modelling tool. *Fractal and Fractional*, 7(8):595, 2023.

[19] D.L. Williams and E.J. Burgess. 34 - hypertension. In D. L. Williams and V. Marks, editors, *Scientific Foundations of Biochemistry in Clinical Practice (Second Edition)*, pages 585–600. Butterworth-Heinemann, 1994.

[20] B.-F. Wu, B.-J. Wu, and C.-P. Hsu. Camera-based blood pressure estimation via windkessel model and waveform features. *IEEE Transactions on Instrumentation and Measurement*, 72:1–13, 2022.